Fluorinated Boronic Acid-Appended Bipyridinium Salts for Diol Recognition and Discrimination via ^{19}F NMR Barcodes

Jörg Axthelm,[†] Helmar Görls,[†] Ulrich S. Schubert,[‡,§] and Alexander Schiller*[,†,§]

[†]Institute for Inorganic and Analytical Chemistry (IAAC), Friedrich Schiller University Jena, Humboldtstrasse 8, D-07743 Jena, Germany

[‡]Institute for Organic Chemistry and Macromolecular Chemistry (IOMC), Friedrich Schiller University Jena, Humboldtstrasse 10, D-07743 Jena, Germany

[§]Jena Center for Soft Matter (JCSM), Friedrich Schiller University Jena, Philosophenweg 7, D-07743 Jena, Germany

Ⓢ *Supporting Information*

ABSTRACT: Fluorinated boronic acid-appended benzyl bipyridinium salts, derived from 4,4′-, 3,4′-, and 3,3′-bipyridines, were synthesized and used to detect and differentiate diol-containing analytes at physiological conditions via ^{19}F NMR spectroscopy. An array of three water-soluble boronic acid receptors in combination with ^{19}F NMR spectroscopy discriminates nine diol-containing bioanalytes—catechol, dopamine, fructose, glucose, glucose-1-phosphate, glucose-6-phosphate, galactose, lactose, and sucrose—at low mM concentrations. Characteristic ^{19}F NMR fingerprints are interpreted as two-dimensional barcodes without the need of multivariate analysis techniques.

Boronic acid-containing molecular probes[1] have been developed as chemosensors for the recognition of diol-containing analytes, such as sugars, nucleotides, catechols, and hydroxyl carboxylic acids.[2−5] Primarily, probes have been generated with the aim to selectively detect glucose *in vivo*.[6] To increase glucose selectivity, the concept of bidentate binding[7] via diboronic acids has been extensively utilized.[8−10] In contrast to the traditional "lock-and-key" approach in carbohydrate detection, differential sensing with multivariate analytical methods represents an attractive alternative.[4,11−16] This technique relies on multiple replicated experiments, and the use of multivariate analysis can be seen as a "black box" calculation with less control over possible false interpretations by non-experts.[15,17] An elegant alternative to reduce complexity is the generation of barcodes without chemometrical methods. Bode et al. discriminated polyols with shape-shifting boronic acids as self-contained sensor arrays.[18] Boronic acid probes are often combined with optical indicators (a fluorophore or chromophore).[3,5,19] However, the intrinsically unselective signals can be exchanged by highly sensitive and discriminative ^{19}F NMR detection.[20−23] Moreover, sensing systems that provide unique and characteristic fingerprints of specific analytes and work at physiological conditions are highly desirable.[24] Herein, we report on an array of water-soluble boronic acid receptors with fluorine probes for sugar recognition and discrimination via two-dimensional (2D) barcodes. The advantages of ^{19}F NMR probes attached to the

reported receptor molecules are the following: direct signaling of the binding event (chemical selectivity of the ^{19}F NMR signals on conjugated sp^2/sp^3 boron); usually, the absence of a background signal; the high sensitivity[25] of non-invasive[19]F NMR spectroscopy (100% natural abundance); the broad chemical shift range of fluorine; and the robustness of receptor−analyte signals against pH changes.[26] Further, the ^{19}F chemical shift is sensitive to minor structural changes in the binding environment.[20,21,24] These favorable characteristics of ^{19}F as an NMR probe let us anticipate that the fluorine substituent would provide a sensitive probe of boron hybridization and structural binding environment of boronic acid receptors for diol-containing analytes.[25,27,28]

We have previously used the fluorescent Singaram—Wessling-type sugar probe[13,29−31] as an allosteric indicator displacement assay for cyanide.[32] In addition, the two-component probe can be described as the molecular logic function "implication" on the few-molecule level of the reporting dye.[33] Concatenated molecular logic gates in large circuits have been demonstrated with a "sugar computer" for arithmetic calculation[33,34] and playing tic-tac-toe.[35]

In this study, three fluorinated boronic acid-appended bipyridinium salts serve as probes for diol-containing (bio)-analyte recognition and discrimination with ^{19}F NMR spectroscopy at physiological conditions. We chose fluorine-labeled boronic acid-appended bipyridinium salts (BBVs) because of their increased selectivity for monosaccharides and solubility in water (up to 5 mM).[13,29] A structural variable is the position of nitrogens in the bipyridyl cores. F-4,4′-*o*-BBV (**1**), F-3,3′-*o*-BBV (**2**), and F-3,4′-*o*-BBV (**3**) were synthesized by *N*-alkylation of corresponding bipyridines via 2-bromomethyl-4-fluorophenyl-boronic acid in dimethylformamide (Scheme 1).[32] Isolation and purification of the products was achieved by precipitation and washing with acetone. X-ray structures of **4** and **5** could be elucidated and are shown in Scheme 1.

Fluorinated boronic acid receptors **1**−**3** comprise two diol binding sites (at boron) and two ^{19}F nuclei as reporters for increased sensitivity[25,28] and selectivity.[13,29] When a diol was added to the receptors in a physiological medium, the boronic acids were converted into boronate esters, inducing an upfield

## Scheme 1. Synthesis Route, Molecule Structures of Receptors 1−3, and the X-ray Structures of 4 and 5[a]
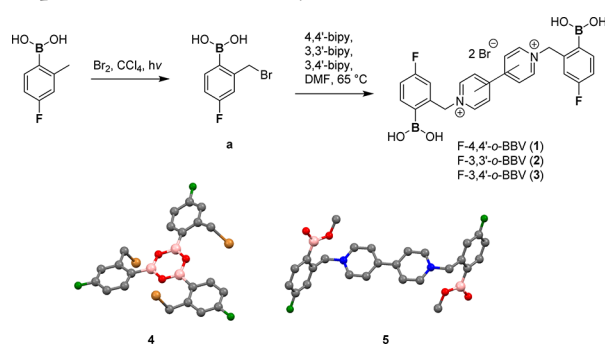
[a]4 is the trimeric anhydride of the precursor a. 5 is the monomethyl ester of the dication of 1. Solvent molecules, bromide anions, and hydrogens are omitted for clarity; gray = carbon, green = fluorine, blue = nitrogen, red = oxygen, pink = boron. For details, see the Supporting Information).

Scheme 2. Illustration of Reversible Boronic Acid−Diol Interaction Recorded with ^{19}F NMR Spectroscopy[a]
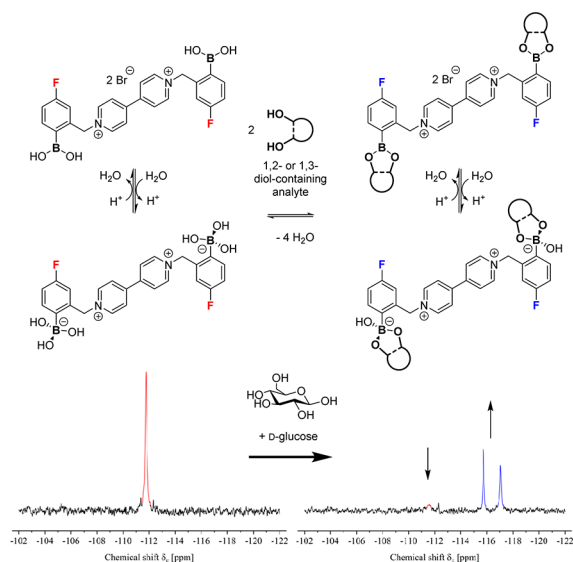

[a]Top, equilibrium of F-4,4′-o-BBV (1) and diol-containing analyte. Bottom, ^{19}F NMR spectra of 1 (4 mM) and with addition of D-glucose (40 mM) in 50 mM phosphate buffer (10% D_2O, pH 7.4), 188 MHz, and 256 scans. Newly appearing and characteristic shifts at δ_F −115.72 and −117.04 ppm belong to the receptor−glucose complex, whereas δ_F −111.76 ppm describes unbound 1.

chemical shift in the ^{19}F NMR spectrum (Scheme 2). For instance, the simple ^{19}F NMR spectrum of 1 (δ_F −111.76 ppm) changes rapidly when D-glucose binds to boron, leading to two new signals at δ_F −115.72 and −117.04 ppm (50 mM phosphate buffer, 10% D_2O, pH 7.4). Multiple possible binding modes were indicated by several peaks (Scheme 2). In the case of reducing sugars, such as D-glucose, that could be explained by the equilibrium of open-ring, α/β-pyranose, and α/β-furanose forms. Binding to 1,2-syn-periplanar OH groups seems to be favored.[9] The intensity and line width of the new signals depended on the binding affinity of the analyte. In general, upfield shifts of approximately δ_F 4−5 ppm with an error of ±0.01 ppm were observed for all analytes.

It is important to note that the receptors 1−3 serve as ^{19}F NMR probes mainly for 1,2-syn-diols at the boron atom[1] over five conjugated bonds within the arene unit. On the NMR time scale, the equilibrium between the boronic acid and the corresponding ester is slow. As a result, the ^{19}F NMR signals of unbound receptor and the formed complexes are well separated. Both sp[2]- and sp[3]-hybridized boron moieties showed relatively broad fluorine peaks in water because of the exchange equilibrium of the boronic acid/ester with their corresponding "ate" complexes compared to samples in DMSO-d_6. Interestingly, the ^{19}F NMR signals of the formed receptor−analyte complexes were not altered by non-interfering buffer media and pH in the measured range of 7−9. Determination of pK_a values of the fluorinated boronic acids has been performed by titration with base and monitored via potentiometry and ^{19}F NMR. Compounds 1−3 displayed lower pK_a values with a drop of 0.2−1 pH unit compared to the non-fluorinated counterparts 4,4′-, 3,3′-, and 3,4′-o-BBV.[29] That result can be explained by the electron-withdrawing effect of fluorine on the boron moiety,[36,37] which enhances diol binding. ^{19}F NMR titration experiments have been performed to determine binding constants of catechol, D-fructose, and D-glucose with 1. In addition, binding constants have been further confirmed by fluorescence experiments due to the fact that 1−3 as dicationic viologen derivatives are quenchers of water-soluble fluorescent dyes, such as anionic pyranine and perylene diimides (see the Supporting Information).[13,29,33]

For ^{19}F NMR sensing experiments, the receptors 1−3 were used in an array to check their cross-reactive sensing potential. Reversible boronic acid−diol interactions were probed in buffered aqueous solution (50 mM HEPES or phosphate buffer, 10% D_2O, pH 7.4) at room temperature. Receptors 1−3 (single receptor solutions, 4 mM each) gave fluorine NMR patterns in the presence of the following bioanalytes: catechol, dopamine, D-fructose, D-glucose, D-glucose-1-phosphate, D-glucose-6-phosphate, D-galactose, D-lactose, and sucrose (40 mM for receptor saturation and high signal-to-noise (S/N) in ^{19}F NMR). However, the limit of detection (LOD) for catechol sensed by F-4,4′-o-BBV (1) is <100 μM at 188 MHz and 1024 scans. The LOD for D-fructose and D-glucose is 200 μM (see the Supporting Information).

In DMSO-d_6, compounds 1 and 2 showed one single peak at δ_F −110.45 and −110.42 ppm, respectively. In contrast, receptor 3 displayed two signals at δ_F −110.49 and −110.54 ppm due to its asymmetry. In buffered aqueous solution, receptor 1 still showed one broad signal at δ_F −111.76 ppm (Figure 1a). In contrast, 2 (δ_F −112.21 ppm) and 3 (δ_F −112.24 and −112.33 ppm) possess signals with smaller intensity at δ_F −111.86 and −111.89 ppm, respectively. This downfield-shifted minor set of signals for 2 and 3 can be tentatively assigned to the free boronic acid form. Broadening of the fluorine peaks in buffered aqueous solution can be explained by the boronic acid−boronate equilibrium (Scheme 2).[1] ^{19}F NMR spectra obtained by screening receptor−diol solutions of 1−3 will be discussed below (Figure 1). With the addition of catechol (Figure 1b) as an aromatic 1,2-diol, all peaks of unbound 1 disappeared, and only one sharp signal at δ_F −116.05 ppm was visible, indicating strong 1:1 boronic acid−catechol esters.[1] The symmetric isomer 2 displayed one sharp signal at δ_F −115.81 ppm, whereas 3 with two diverse ^{19}F nuclei produced two sharp signals at δ_F −115.92 and −116.09 ppm. Interestingly, the similar neurotransmitter dopamine (Figure 1c) can be discriminated from catechol with the shift
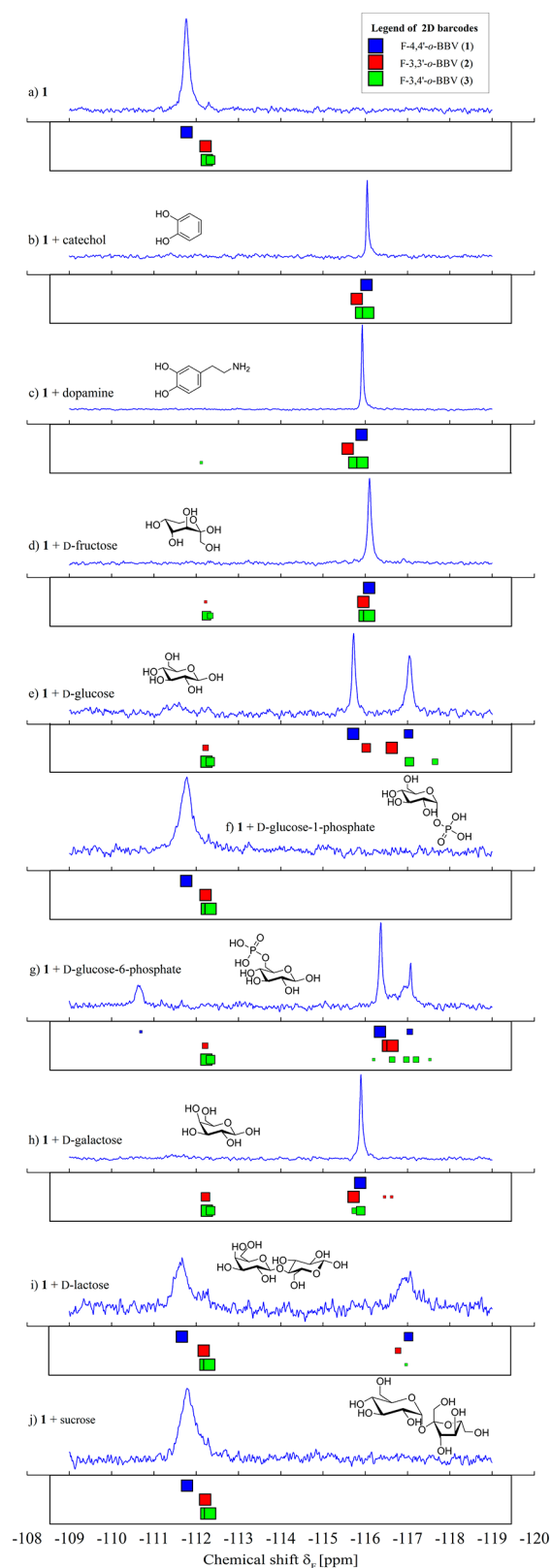
Figure 1. ^{19}F NMR spectra of **1** with diol and 2D barcodes of the array **1**−**3**. 2D barcodes underneath each spectrum relate to the receptors **1**, **2**, and **3** (blue, red, and green) and diol, respectively. Conditions: **1**−**3** (4 mM), diol (40 mM) in 50 mM phosphate buffer (10% D_2O, pH 7.4), room temperature, 188 MHz, and 256 scans.

change significantly above the experimental error. The presence of an ethylamine group on dopamine induced significantly

shifted ^{19}F peaks with **1** (δ_F −115.93 ppm), **2** (δ_F −115.60 ppm), and **3** (δ_F −115.76 and −115.95 ppm). The complexity of ^{19}F NMR signals of **1**−**3** was further demonstrated with a selection of mono- and disaccharides: D-fructose (Figure 1d), which is known for its strong affinity to boronic acids,[1,2] yields one sharp receptor−analyte peak at δ_F −116.10 ppm with **1** and −115.97 ppm with **2** (δ_F −116.00 and −116.11 ppm for **3**). In contrast, D-glucose (Figure 1e), typically difficult to discriminate from D-fructose, generated two peaks with **1** at δ_F −115.72 and −117.04 ppm. Two binding peaks were also observed for **2** (δ_F −116.04 and −116.65 ppm) and **3** (δ_F −116.68 and −117.07 ppm). However, the smaller affinity of D-glucose was displayed by the presence of unbound receptor species. In addition, binding constants have been determined via ^{19}F NMR and fluorescence quenching.[29] For D-fructose and D-glucose, the apparent K_b values from the two techniques are similar, within the same order of magnitude. However, K_b values for all analytes have been compared from the fluorescence quenching (Table S3 in the Supporting Information). Receptor **1** and 4,4′-o-BBV[29] show very similar binding constants, ranging over two orders of magnitude (D-fructose with **1**, 1692 M^{-1}; **2**, 210 M^{-1}; and **3**, 142 M^{-1}). Also the K_b values for D-glucose (**1**, 45 M^{-1}; **2**, 16 M^{-1}; **3**, not determinable) follow the trend of decreasing affinity. However, receptor **2** displays higher affinities for D-glucose-6-phosphate and galactose (Table S3). D-galactose (Figure 1h), with one strong ^{19}F signal at δ_F −115.90 ppm with **1**, shows good affinity compared to **2** (δ_F −115.74, −116.48, and −116.65 ppm) and **3** (δ_F −115.77 and −115.91 ppm). D-Lactose (Figure 1i) displays only a broad signal with **1** at δ_F −117.07 ppm. Overall, the strongest affinity for all analytes within the ^{19}F NMR assay was monitored with the 4,4′-isomer **1**. Very weak to no affinities to all receptors were measured with the control substrates D-glucose-1-phosphate (Figure 1f) and the disaccharide sucrose (Figure 1j). Non-reducing sugars rarely bind to boronic acids.[13,38] All ^{19}F NMR sensing experiments and data of **1**−**3** are given in the Supporting Information.

At this point one discrete fluorinated boronic acid of the collection **1**−**3** would be able to discriminate only some few sugars. Thus, we collected the information for all three receptors in an array. We refrained from using multivariate analysis because we wanted to establish an easier and more intuitive way to read out the data. Thus, the ^{19}F NMR spectra of **1**−**3** with the set of diol-containing bioanalytes were transferred into a 2D barcode (Figure 1). For this purpose, chemical shifts and intensities were extracted from all spectra. The barcode uses NMR shifts in ppm units. Thresholds at 25, 50, and 75% of relative intensity of the peaks produce barcode squares, such as quick response (QR) codes, at corresponding shift values. The peak intensity is reflected by the corresponding size of the colored squares. Originally, the two-dimensional QR Code system was invented by the automotive industry (Toyota, Denso-Wave, http://www.qrcode.com/en/) to take advantage of its fast readability and greater storage capacity compared to standard barcodes. Today, QR Codes are applied in product tracking, item identification, time tracking, and document management. Our 2D barcodes can be used to visualize and conveniently compare the interaction of an array of boronic acid receptors with a set of diol-containing analytes. The square patterns resulted from ^{19}F NMR signals of bound and unbound receptors. Further variance is given by the different sizes of the colored squares. In this combination, the patterns of D-fructose (Figure 1d), D-

glucose (Figure 1e), D-glucose-6-phosphate (Figure 1g), D-galactose (Figure 1h), and D-lactose (Figure 1i) can be easily differentiated by the naked eye. In contrast, only receptor **1** alone and its corresponding blue patterns with catechol (Figure 1b), dopamine (Figure 1c), D-fructose (Figure 1d), and D-galactose (Figure 1h) hamper discrimination among the mentioned analytes. This demonstrates the importance of combining several boronic acid receptors in an array to provide successful differentiation. In addition, magnetically diverse ^{19}F nuclei in receptor **3** add a more complex and better discriminable sub-pattern to the array (e.g., with D-glucose (Figure 1e), D-glucose-6-phosphate (Figure 1g), and D-galactose (Figure 1h)). However, symmetric ^{19}F probes, such as receptors **1** and **2**, are necessary for their increased binding affinity. It is also important to demonstrate the limits of the 2D barcodes. D-Glucose-1-phosphate and sucrose, which are not binding to our receptors under the present conditions, display patterns very similar to those of the unbound receptors (Figure 1a,f,j). Visual discrimination of catechol (Figure 1b) and dopamine (Figure 1c) is also difficult; however, the ^{19}F NMR shifts are clearly separated. Further parameters from the ^{19}F NMR signals, such as line widths, S/N values, or the fine-tuning of our discriminatory grid, and of course the addition of further possible receptor scaffolds could be used to generate stronger variance for improved discrimination in the future.

In summary, we present a new approach using three fluorinated boronic acid-appended bipyridinium salts and ^{19}F NMR spectroscopy for the detection and discrimination of diol-containing analytes in aqueous buffer solution via 2D barcodes. The concept can be widened by screening other analyte classes, monitoring enzyme reactions,[39] and applying this technique in magnetic resonance imaging.

■ ASSOCIATED CONTENT

Ⓢ Supporting Information
The Supporting Information is available free of charge on the ACS Publications website at DOI: 10.1021/jacs.5b10934.

> Experimental procedures and characterization data for all new compounds (PDF)
> X-ray crystallographic data for **4** and **5** (CIF)

■ AUTHOR INFORMATION

Corresponding Author
*alexander.schiller@uni-jena.de

Notes
The authors declare no competing financial interest.

■ ACKNOWLEDGMENTS

■ REFERENCES

(1) Hall, D. G. *Boronic Acids*; Wiley-VCH: Weinheim, 2011.

(2) Nishiyabu, R.; Kubo, Y.; James, T. D.; Fossey, J. S. *Chem. Commun.* **2011**, *47*, 1106.

(3) Wu, J.; Kwon, B.; Liu, W.; Anslyn, E. V.; Wang, P.; Kim, J. S. *Chem. Rev.* **2015**, *115*, 7893.

(4) You, L.; Zha, D.; Anslyn, E. V. *Chem. Rev.* **2015**, *115*, 7840.

(5) de Silva, A. P.; Gunaratne, H. Q. N.; Gunnlaugsson, T.; Huxley, A. J. M.; McCoy, C. P.; Rademacher, J. T.; Rice, T. E. *Chem. Rev.* **1997**, *97*, 1515.

(6) Cunningham, D. D.; Stenken, J. A. *In Vivo Glucose Sensing*; Wiley: Hoboken, 2010.

(7) Robertson, A.; Shinkai, S. *Coord. Chem. Rev.* **2000**, *205*, 157.

(8) James, T. D.; Sandanayake, S.; Shinkai, S. *Angew. Chem., Int. Ed. Engl.* **1994**, *33*, 2207.

(9) Norrild, J. C.; Eggert, H. *J. Am. Chem. Soc.* **1995**, *117*, 1479.

(10) Huang, Y.-J.; Ouyang, W.-J.; Wu, X.; Li, Z.; Fossey, J. S.; James, T. D.; Jiang, Y.-B. *J. Am. Chem. Soc.* **2013**, *135*, 1700.

(11) Rout, B.; Milko, P.; Iron, M. A.; Motiei, L.; Margulies, D. *J. Am. Chem. Soc.* **2013**, *135*, 15330.

(12) Schiller, A.; Vilozny, B.; Wessling, R. A.; Singaram, B. *Anal. Chim. Acta* **2008**, *627*, 203.

(13) Schiller, A.; Wessling, R. A.; Singaram, B. *Angew. Chem., Int. Ed.* **2007**, *46*, 6457.

(14) Musto, C. J.; Suslick, K. S. *Curr. Opin. Chem. Biol.* **2010**, *14*, 758.

(15) Anzenbacher, J. P., Jr.; Lubal, P.; Bucek, P.; Palacios, M. A.; Kozelkova, M. E. *Chem. Soc. Rev.* **2010**, *39*, 3954.

(16) Kostereli, Z.; Scopelliti, R.; Severin, K. *Chem. Sci.* **2014**, *5*, 2456.

(17) Anslyn, E. V. *J. Org. Chem.* **2007**, *72*, 687.

(18) Teichert, J. F.; Mazunin, D.; Bode, J. W. *J. Am. Chem. Soc.* **2013**, *135*, 11314.

(19) Wang, W.; Gao, X.; Wang, B. *Curr. Org. Chem.* **2002**, *6*, 1285.

(20) Zhao, Y.; Swager, T. M. *J. Am. Chem. Soc.* **2013**, *135*, 18770.

(21) Zhao, Y.; Swager, T. M. *J. Am. Chem. Soc.* **2015**, *137*, 3221.

(22) Smith, G. A.; Hesketh, R. T.; Metcalfe, J. C.; Feeney, J.; Morris, P. G. *Proc. Natl. Acad. Sci. U. S. A.* **1983**, *80*, 7178.

(23) Gan, H.; Oliver, A. G.; Smith, B. D. *Chem. Commun.* **2013**, *49*, 5070.

(24) Zhao, Y.; Markopoulos, G.; Swager, T. M. *J. Am. Chem. Soc.* **2014**, *136*, 10683.

(25) London, R. E.; Gabel, S. A. *J. Am. Chem. Soc.* **1994**, *116*, 2562.

(26) Chen, H.; Viel, S.; Ziarelli, F.; Peng, L. *Chem. Soc. Rev.* **2013**, *42*, 7971.

(27) Yeste, S. L.; Powell, M. E.; Bull, S. D.; James, T. D. *J. Org. Chem.* **2009**, *74*, 427.

(28) Iannazzo, L.; Benedetti, E.; Catala, M.; Etheve-Quelquejeu, M.; Tisne, C.; Micouin, L. *Org. Biomol. Chem.* **2015**, *13*, 8817.

(29) Gamsey, S.; Miller, A.; Olmstead, M. M.; Beavers, C. M.; Hirayama, L. C.; Pradhan, S.; Wessling, R. A.; Singaram, B. *J. Am. Chem. Soc.* **2007**, *129*, 1278.

(30) Suri, J. T.; Cordes, D. B.; Cappuccio, F. E.; Wessling, R. A.; Singaram, B. *Angew. Chem., Int. Ed.* **2003**, *42*, 5857.

(31) Vilozny, B.; Schiller, A.; Wessling, R. A.; Singaram, B. *J. Mater. Chem.* **2011**, *21*, 7589.

(32) Jose, D. A.; Elstner, M.; Schiller, A. *Chem. - Eur. J.* **2013**, *19*, 14451.

(33) Elstner, M.; Weisshart, K.; Müllen, K.; Schiller, A. *J. Am. Chem. Soc.* **2012**, *134*, 8098.

(34) Elstner, M.; Axthelm, J.; Schiller, A. *Angew. Chem., Int. Ed.* **2014**, *53*, 7339.

(35) Elstner, M.; Schiller, A. *J. Chem. Inf. Model.* **2015**, *55*, 1547.

(36) Sharrett, Z.; Gamsey, S.; Fat, J.; Cunningham-Bryant, D.; Wessling, R. A.; Singaram, B. *Tetrahedron Lett.* **2007**, *48*, 5125.

(37) Brzozowska, A.; Ćwik, P.; Durka, K.; Kliś, T.; Laudy, A. E.; Luliński, S.; Serwatowski, J.; Tyski, S.; Urban, M.; Wróblewski, W. *Organometallics* **2015**, *34*, 2924.

(38) Dowlut, M.; Hall, D. G. *J. Am. Chem. Soc.* **2006**, *128*, 4226.

(39) Vilozny, B.; Schiller, A.; Wessling, R. A.; Singaram, B. *Anal. Chim. Acta* **2009**, *649*, 246.